PROTEINS
STRUCTURE ■ FUNCTION ■ BIOINFORMATICS

The osmolyte betaine promotes protein misfolding and disruption of protein aggregates

Antonino Natalello,[1,2] Jing Liu,[3] Diletta Ami,[4] Silvia Maria Doglia,[1,2] and Ario de Marco[4]*

[1] Department of Biotechnology and Biosciences, University of Milano-Bicocca, Piazza della Scienza 2, Milan 20126, Italy
[2] Consorzio Nazionale Interuniversitario per le Scienze Fisiche della Materia (CNISM) UdR Milano-Bicocca, Via Cozzi 53, Milan 20125, Italy
[3] Key Laboratory of Ion Beam Engineering, Chinese Academy of Sciences, Hefei 230031, Anhui, People's Republic of China
[4] COGENTECH, via Adamello 16, Milan 20139, Italy

ABSTRACT

In this work the effect of betaine on the structure and aggregation of the GST-GFP fluorescent fusion protein was studied by different complementary techniques, including electron microscopy, dynamic light scattering, circular dichroism, and FTIR spectroscopy. Although osmolytes are known to be protein stabilizers *in vivo*, the effect of betaine on the structure and aggregation of our model protein was found to be strictly concentration dependent. We demonstrated that, by changing betaine concentration, it was possible to tune the formation of protein soluble assemblies and insoluble aggregates, as well as to disaggregate preformed aggregates. In particular, at a critical concentration of betaine between 5 and 7.5 m*M*, the protein precipitated into macroscopic prefibrillar structures, rich in intermolecular β-sheets, which were found to bind thioflavine T and to be inaccessible to protease. Instead, at higher betaine concentration (10–20 m*M*) the misfolded protein lost its fluorescence, but formed soluble assemblies with hydrodynamic radius of about 16 nm. These structures displayed a reduced propensity to further aggregate under thermal treatment. In addition, betaine at this high concentration was also found to disrupt large preformed aggregates, obtained under different conditions, into protein soluble assemblies. It is the first time that a disaggregation process has been described for a chemical chaperone. A mechanism for the betaine concentration-dependent effect on protein misfolding, aggregation, and disaggregation is proposed and its possible physiological implications are discussed.

Proteins 2009; 75:509–517.

Key words: aggregation; circular dichroism; disaggregation; dynamic light scattering; Fourier transform infrared spectroscopy; oligomers; osmolytes; protein destabilization; protein stability.

INTRODUCTION

Osmolytes are small organic molecules that cells accumulate in response to environmental stress in order to preserve protein stability and to equilibrate cellular osmotic pressure.[1] Because of their potential protective role toward protein misfolding and aggregation, osmolyte applications in medicine and biotechnology have been considered. Indeed, protein misfolding and aggregation have been found to be involved in the development of several neurodegenerative pathologies, like Alzheimer's, Huntington's, Parkinson's, amyotrophic lateral sclerosis, and prion disease.[2] In biotechnology, heterologous protein productions often lead to the aggregation of the overexpressed protein in form of inclusion bodies.[3,4] The study of these aggregation processes has been extensively performed both in physiological conditions and in heterologous systems, using effectors able to modulate protein aggregation.[3–10] However, the role of osmolytes in these processes is still not completely understood, since these molecules were found not only to inhibit[11–13] but also to induce protein aggregation.[14–16]

In this article, the effect of the osmolyte betaine on the structure and aggregation of the model protein GST-GFP[3] has been studied by several complementary biochemical and biophysical techniques. Betaine is a compatible solute that stabilizes proteins during stress conditions *in vivo* and for this reason has been proposed for biotechnological and therapeutic applications.[17–20] Here we show that betaine, depending on its concentration, can either induce protein aggregation or disrupt preformed large aggregates. This unexpected result indicates

Abbreviations: CD, circular dichroism; DLS, dynamic light scattering; EM, electron microscopy; FTIR, Fourier transform infrared; GST-GFP, glutathione-S-transferase-green fluorescent protein; Rh, hydrodynamic radius; TEV, tobacco etch virus; ThT, thioflavin T.

The authors have no conflict of interests.
Grant sponsor: Fondo di Ateneo per la Ricerca (FAR).
*Correspondence to: Ario de Marco, IFOM-IEO Campus for Oncogenomics, via Adamello 16, Milan 20139, Italy. E-mail: ario.demarco@ifom-ieo-campus.it.
Received 2 May 2008; Revised 11 July 2008; Accepted 28 August 2008
Published online 10 September 2008 in Wiley InterScience (www.interscience.wiley.com).
DOI: 10.1002/prot.22266

that osmolytes not only prevent protein misfolding and aggregation, but they behave as molecular chaperones in the active disruption of aggregates.[21,22]

MATERIALS AND METHODS

Cell growth and protein handling

The fusion construct His-GST-GFP was transformed in BL21 (DE3) RIL codon plus[23] and its overnight expression at 20°C was induced by 0.1 m*M* IPTG. The bacteria were pelleted, washed in 10 mL of PBS, and finally stored at 20°C.

The pellet was resuspended in 10 mL of lysis-buffer (50 m*M* Tris-HCl, pH 8.0, 0.5*M* NaCl, 5 m*M* $MgCl_2$, 1 mg/mL lysozyme, 10 μg/mL DNase), sonicated in a water bath (Branson 200) for 5 min, and the lysate was incubated for 30 min at room temperature with constant rocking. The supernatant was recovered after ultracentrifugation (35 min at 150,000*g*) and loaded on a HiTrap chelating affinity column connected to a FPLC instrument (Amersham Biosciences) pre-equilibrated with 20 m*M* Tris HCl, pH 7.8, 500 m*M* NaCl, 15 m*M* imidazole. His-tagged GST-GFP was eluted in 20 m*M* Tris, pH 8.0, 125 m*M* NaCl, and 250 m*M* imidazole; desalted in 20 m*M* Tris HCl, pH 8.0, 1 m*M* EDTA, 1 m*M* DTT, and 5% glycerol; and filtered before storage. Its concentration was quantified using its extinction coefficient and the absorbance at 280 nm. Proteolysis experiments were performed incubating 10 μg tobacco etch virus (TEV) protease × 1 mg GST-GFP for 2 h at 30°C. Digested proteins were separated by standard SDS-PAGE.

Electron microscopy

GST-GFP samples were collected from the precipitates or the suspensions, whenever no visible aggregate was detectable.

The material was fixed by dropping 5 μL of each protein sample on a grid (Agar Scientific) and was incubated 1 min at room temperature. The excess fluid was removed using filter paper and the unbound protein was washed before the grids were placed on a 50 μL drop of 1% uranyl acetate with the section side downwards. Finally, the grids were dried, placed in the grid-chamber, and stored in desiccators before observation with a CM120 BioTwin electron microscope (Philips).

Sucrose gradient analysis

The aggregates, formed after betaine addition to 4.5 μ*M* of purified GST-GFP, were separated using a sucrose step gradient formed by four layers of 20 m*M* TrisHCl buffer, pH 8, and 50 m*M* NaCl containing 80, 70, 50, 30, and 0% sucrose, respectively. The tubes were centrifuged 15 h at 180,000*g* at 4°C using a SW40Ti rotor and a L-70 Beckman ultracentrifuge. Sucrose fractions were recovered separately and protein content estimated by the absorbance at 280 nm, using GST-GFP extinction coefficient.

Fluorescence measurements

The intrinsic fluorescence of the protein samples (9 μ*M*) was studied by exciting them at 295 nm and recording the emission spectra in the region between 310 and 420 nm.

The aggregation index[24] of GST-GFP (in 20 m*M* TrisHCl buffer, pH 8) was evaluated recording scattered light at 280 nm and emission light between 260 and 400 nm.

The interaction of protein aggregates (3 μ*M* GST-GFP) with Thioflavine T (ThT), a well-known marker of amyloids,[25] was determined by fluorescence measurements with excitation at 450 nm and emission at 482 nm.

The fluorescence measurements were performed using an AB2 Luminescence Spectrometer (Aminco Bowman Series 2) equipped with SLM 4 software and a J-810 spectrofluorimeter (Jasco).

Circular dichroism spectroscopy

Protein secondary and tertiary structures were studied by CD spectroscopy. For the far-UV (200–250 nm), GST-GFP at 9 μ*M*, in 20 m*M* TrisHCl buffer, pH 8, was measured using a cuvette with optical path of 1 mm (Hellma). For the near-UV (250–300 nm), the protein at 36 μ*M* was measured by using a cuvette with optical path of 1 cm (Hellma). For samples containing different concentrations of betaine, measurements were performed after 1 h incubation at room temperature. CD spectra were recorded with a Jasco J-810 spectropolarimeter (Jasco) under the following conditions: 20 nm/min scan speed; 3 nm band width, and three accumulations.

Dynamic light scattering and turbidity analyses

Dynamic light scattering (DLS) measurements were performed at room temperature on samples at 9 and 36 μ*M* GST-GFP protein (in 20 m*M* TrisHCl buffer, pH 8) and at different betaine concentrations. A DynaPro 99 (Protein Solutions) instrument was employed. The analysis was performed by the Dynamics 5.20.05 software (Protein Solutions).

Turbidity was evaluated by recording the absorbance at 340 nm.

Fourier transform infrared spectroscopy

For the measurements of the infrared absorption spectra, GST-GFP samples were prepared in 20 m*M* TrisHCl buffer, pH 8, at a concentration of 120 μ*M*. Betaine was added to the protein solution at different final concentra-

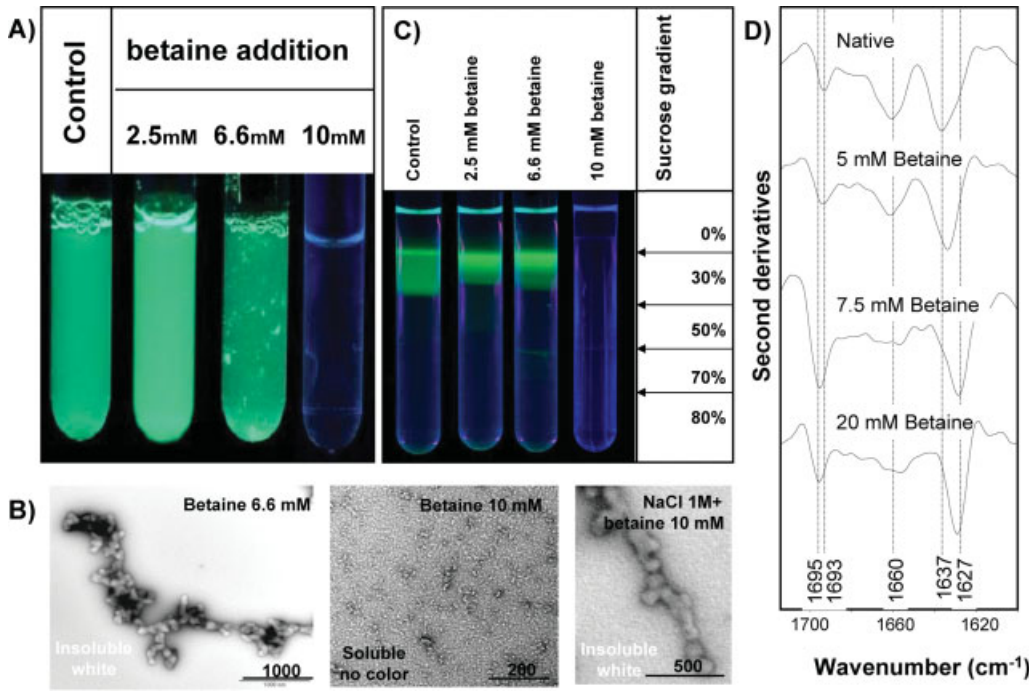

Figure 1

Aggregation patterns of GST-GFP in the presence of increasing betaine concentrations. **A**: GST-GFP (3 μ*M*) was incubated in the presence of betaine at 2.5, 6.6, and 10 m*M*. **B**: EM images of GST-GFP (1.5 μ*M*) incubated in the presence of 6.6, 10 m*M* betaine, and 10 m*M* betaine with 1 *M* NaCl. **C:** Sucrose step-gradient analysis of GST-GFP (4.5 μ*M*) preincubated in the presence of 2.5, 6.6, and 10 m*M* betaine. **D:** Second derivative of FTIR spectra of GST-GFP (120 μ*M*) incubated in the presence of 5, 7.5, 20 m*M* betaine. Spectra normalization at the 1516 cm^{-1} tyrosine band was performed to compensate for possible differences in protein content. The band peak positions are indicated.

tions from 0 to 20 m*M*. Two hours after the addition of betaine at room temperature, a solution volume of about 15 μL was deposited on a BaF_2 support and dried for 20 min at room temperature. The protein hydrated film was then rinsed by adding 200 μL of Tris-HCl buffer to reduce the contribution of free betaine in the spectrum, gently removing the excess fluid using an absorbing filter paper.

The FTIR absorption spectra of protein hydrated films were measured in transmission using the infrared microscope UMA500 coupled to the FTS40-A spectrometer (both from Digilab, USA).

Through the microscope's variable aperture, ranging from 100 μm × 100 μm to 200 μm × 200 μm, selected areas of the protein film were measured under the following conditions: 2 cm^{-1} spectral resolution, 20 kHz scan speed, 256 scan co-additions, triangular apodization. A nitrogen cooled MCT detector was employed. Both microscope and spectrometer were carefully purged with dry air.

For the data analysis, the second derivative absorption spectra were obtained by a Savitzky-Golay algorithm (5 points), after an 11 points binomial smoothing of the measured spectra, using Grams/AI software (Thermogalactic, USA).

RESULTS

Concentration dependent effects of betaine on GST-GFP misfolding and aggregation

The fluorescent GST-GFP fusion protein (glutathione S-transferase-green fluorescent protein) has been proved to be a useful model system to study the complexity of the recombinant aggregation patterns in bacteria.[3,26] Here, we report the effects of the osmolyte betaine on GST-GFP structure and aggregation.

GST-GFP at a concentration of 3 μ*M* was first incubated with increasing amounts of betaine, to evaluate—by naked-eye inspection of the sample—the green fluorescence of the protein and the possible formation of macroscopic aggregates [Fig. 1(A)]. Low betaine concentrations (1–2.5 m*M*) did not apparently influence the protein sample, but the addition of 5–7.5 m*M* betaine resulted in the flocculation of part of the protein solution into white bodies. These precipitates were found to bind thioflavine T (ThT), a well-known marker of amyloid-like structures (Table I),[25] and appeared to be made by large prefibrillar structures, when observed by EM [Fig. 1(B)].

When 10 m*M* betaine was added, the protein lost its fluorescence, but did not precipitate [Fig. 1(A)]. Only tiny spherical bodies were observed by EM in the protein

Table I
Functional and Structural Properties of the GST-GFP Fusion Protein in the Presence of Different Betaine Concentrations

Method of analysis	Native GST-GFP (no betaine)	GST-GFP + betaine (5–7.5 m*M*)	GST-GFP + betaine (10–20 m*M*)
Naked eye inspection	Green solution	Insoluble white aggregates	Uncolored solution, no precipitates
Mass distribution in sucrose gradient	0% sucrose: green (100% protein)	0% sucrose: green (80% protein) 50–70% sucrose: uncolored (20% protein)	0% sucrose: uncolored (100% protein)
Morphology by EM	No aggregates	Chain-like aggregates	Tiny spherical aggregates
Aggregation index	~0.5	>10	~0.5
ThT fluorescence (A.U.)	100	341	128
Size distribution by DLS (Rh)	4.2 nm	50.2 nm; >3,000 nm	16.0 nm
Tertiary structure: Trp fluorescence	λ_{em} 340 nm	—	λ_{em} 345 nm (more solvent exposed)
Tertiary structure: Near-UV CD	Native-like tertiary structure	—	Unfolded tertiary structure
Secondary structures: Far-UV CD	Native α-helices and β-sheets	—	Partial unfolding
Secondary structures: FTIR	Native α-helices and β-sheets	Intermolecular β-sheets	Intermolecular β-sheets
TEV protease accessibility	Yes	No	Yes
Aggregation by thermal treatments	Yes	—	Protection from aggregation

CD, circular dichroism; DLS, dynamic light scattering; EM, electron microscopy; FTIR, Fourier transform infrared; GST-GFP, glutathione-S-transferase-green fluorescent protein; Rh, hydrodynamic radius; ThT, thioflavin T.

solution at this betaine concentration [Fig. 1(B)]. Incubation of GST-GFP in the presence of both 1*M* NaCl and 10 m*M* betaine resulted in an accelerated precipitation of white aggregates with a rod-like structure [Fig. 1(B)], indicating that salt promoted the aggregation of betaine-induced misfolded intermediates.

Before all the biochemical and biophysical characterizations reported below, the concentration dependent effect of betaine on GST-GFP was checked by the naked eye inspection of the samples. Therefore, this simple experiment [Fig. 1(A)] was performed more than 30 times, working on different protein preparations and betaine batches.

The presence of aggregates in solution was estimated measuring the ratio between light scattering at 280 nm and the fluorescence emission of the protein aromatic residues at 340 nm. Such "aggregation index"[24] was measured after the incubation of GST-GFP in the presence of 2.5, 6.6, and 10 m*M* betaine. The control (GST-GFP protein without betaine) showed an aggregation index close to 0.5 and a similar value was measured using the samples treated with 2.5 and 10 m*M* betaine. These values indicate a low level of aggregation of the GST-GFP protein.[3] Only the sample treated with 6.6 m*M* betaine appeared highly aggregated, displaying an aggregation index higher than 10.

Structural characterization of GST-GFP in native, misfolded, and aggregated forms

The concentration-dependent effect of betaine on GST-GFP was further investigated by several biophysical techniques.

GST-GFP size distribution evaluated by sucrose gradient analysis

To separate aggregates of increasing complexity,[3] GST-GFP (4.5 μ*M*) preincubated with betaine at different concentrations for 1 h was centrifuged through a sucrose gradient. As shown in Figure 1(C), in the absence and in the presence of betaine at 2.5 and 6.6 m*M*, the large fluorescent band at the top of the sucrose gradient is due to GST-GFP in its soluble form. A further band, at the interface between 50 and 70% sucrose, is visible only in the fraction treated with 6.6 m*M* betaine, indicating the presence of aggregates with larger mass and weak fluorescence.[3] The GST-GFP content in each band was estimated by recovering the sucrose fractions and measuring their absorption at 280 nm using an extinction coefficient $\epsilon = 67917.5\ M^{-1}\ cm^{-1}$. Under these conditions, the band at the 50–70% sucrose interface represented ~20% of the total protein. At 10 m*M* betaine no fluorescent bands were observed in the sucrose gradient, as expected from the data of Figure 1(A), and all the protein remained at the top of the gradient.

GST-GFP size distribution determined by dynamic light scattering and turbidity

The size of protein aggregates in the presence of different betaine concentrations were studied by DLS (Table I) and turbidity measurements (absorbance at 340 nm). DLS analysis of the control GST-GFP showed the presence of particles with hydrodynamic radius (Rh) of

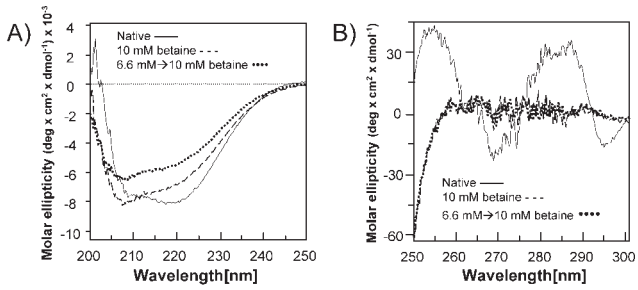

C)

	GST-GFP 0 mM Betaine	→ GST-GFP 6.6 mM Betaine	→ GST-GFP 10 mM Betaine
Naked eye inspection	Green solution	White aggregates	Transparent solution
DLS/Rh	4.2 nm	50-3000 nm	22.9 nm
Turbidity [$OD_{340\ nm}$]	0.058	0.754	0.058

Figure 2

Secondary and tertiary structure of GST-GFP in the presence of different betaine concentrations. **A:** Far-UV CD spectra of native 9 μ*M* GST-GFP (continuous) and in the presence of 10 m*M* betaine (broken line). At 6.6 m*M* betaine, protein precipitation was induced. These aggregates were dissolved by addition of betaine up to 10 m*M*, and their CD spectrum (dotted) was then measured. **B:** Near-UV CD spectra of GST-GFP (36 μ*M*) as in A. **C:** Naked eye inspection, dynamic light scattering (DLS), and turbidity of: native GST-GFP (9 μ*M*); GST-GFP (9 μ*M*) in the presence of 6.6 m*M* betaine; GST-GFP (9 μ*M*) after addition of betaine up to 10 m*M*, to preformed protein aggregates at 6.6 m*M* betaine.

4.2 nm, due to GST-GFP dimers. The protein displayed green fluorescence [Fig. 1(A)] and a turbidity of 0.058. The addition of 6.6 m*M* betaine induced the immediate precipitation of white aggregates and an increase of the turbidity up to 0.754. DLS analyses of the soluble fraction gave an average Rh of 52 nm, while DLS measurements, performed immediately after the resuspension of precipitates, show the presence of particles with Rh larger than 3000 nm. When 36 μ*M* GST-GFP was incubated for 1 h with 6.6 m*M* betaine, the DLS analysis indicated that all the protein was in the form of large aggregates.

After 10 m*M* betaine addition, the sample became transparent, its turbidity value was similar to that of the control, and the Rh of the particles in suspension was around 16 nm (Table I). However, the protein remains unfolded, as inferred by the lack of GFP fluorescence and by the CD spectra (Table I).

GST-GFP secondary and tertiary structures detected by circular dichroism

The secondary and tertiary structures of GST-GFP were studied by CD.[27] The CD analysis in the far-UV region (200–250 nm) in the absence of betaine reflected the presence of α-helix and β-sheet secondary structures in the native GST-GFP protein [Fig. 2(A)]. Under the same conditions, the presence of native-like tertiary structure was verified by CD in the near-UV region (250–300 nm) [Fig. 2(B)]. At 2.5 m*M* betaine the CD spectra (not shown) coincided with that of the native protein. At 6.6 m*M* betaine the massive aggregation of GST-GFP impaired the CD measurements. After incubation with 10 m*M* betaine, far-UV and near-UV CD spectra indicated, respectively, a partial unfolding of the GST-GFP secondary structures and the loss of the protein tertiary structure [Fig. 2(A,B)].

GST-GFP tertiary structure by tryptophan fluorescence

In the absence of betaine, the fluorescence emission maximum of GST-GFP tryptophans, excited at 295 nm, was found to be around 340 nm, indicating that several tryptophans are already solvent exposed in the native protein. After protein incubation with 10 m*M* betaine, the fluorescence emission shifted toward higher wavelengths (345 nm). This result indicates that tryptophans become more exposed to the solvent in presence of 10 m*M* betaine.

Betaine induced unfolding and aggregation of GST-GFP studied by FTIR spectroscopy

FTIR spectroscopy enables to obtain information on the secondary structure, unfolding, and aggregation of proteins.[28–30] The infrared absorption spectrum of native GST-GFP in form of hydrated film was measured in transmission by FTIR microspectroscopy[31] in the Amide I region (1700 to 1600 cm^{-1}) where the absorption of the C=O peptide group allows the identification of the secondary elements of the protein.[32,33] For these FTIR measurements, protein at a concentration one order of magnitude higher than that in the above experiments is required. Consequently, the critical betaine concentrations affecting the GST-GFP structure were also increased, namely, to 7.5 m*M* to induce protein precipitation and to 20 m*M* to obtain the loss of green fluorescence in absence of protein precipitation.

The second derivative spectrum in the Amide I region of native GST-GFP is reported in Figure 1(D). The component around 1660 cm^{-1} can be assigned mainly to the α-helical structures[33] of the GST moiety and the two components around 1693 and 1637 cm^{-1} principally to the GFP antiparallel β-sheet structures,[33] in agreement with the crystallographic data of the two fused proteins.[34,35]

The infrared spectrum in the presence of 5 m*M* betaine shows that most of the protein keeps its α-helix and β-sheet structures. After the addition of 7.5 m*M* betaine to the protein solution, GST-GFP immediately aggregates into macroprecipitates. The FTIR spectrum of these aggregates shows the loss of native secondary structure and the presence of the two intermolecular β-sheet marker bands of aggregation at 1627 and 1695 cm^{-1}. A peculiar feature of this spectrum is the relative intensity of the two intermolecular β-sheet components with the 1695 cm^{-1} band unusually intense, as can be seen by comparison with that of the thermal aggregate spectra.[10,30,36,37]

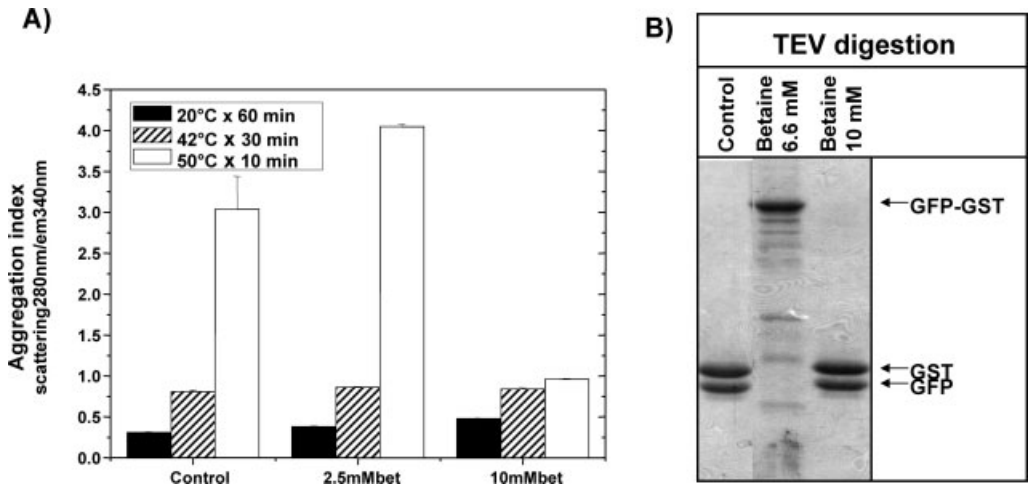

Figure 3

Betaine effect on GST-GFP stability. **A:** Aggregation index of GST-GFP (6 μ*M*) in the absence of betaine and in the presence of 2.5 and 10 m*M* betaine, incubated at 42 and 50°C. **B:** TEV protease digestion of the GST-GFP preincubated with 6.6 and 10 m*M* betaine.

The protein in solution lost its fluorescence when 20 m*M* betaine was added, but no visible precipitates were recovered even after centrifugation. No native secondary structure was observed in the FTIR spectrum. However, when comparing the spectra of betaine-induced aggregates, small but significant differences can be appreciated. At 20 m*M* betaine, the band around 1695 cm^{-1} became less intense than at 7.5 m*M* and a minor shift in peak position was observed for the low frequency aggregate band from 1627 to 1628 cm^{-1}.

Betaine effect on GST-GFP thermal aggregation

The GST-GFP thermal stability and aggregation in the presence of increasing concentrations of betaine was evaluated measuring the aggregation index (AI)[24] of the protein solution incubated at different temperatures [Fig. 3(A)]. GST-GFP formed thermal aggregates when incubated at 50°C in the absence of betaine as indicated by a value of AI ~3. We observed that the addition of 2.5 m*M* betaine had no protective effects against thermal aggregation, while, as reported above, 6.6 m*M* betaine induced protein precipitation at all temperatures (data not shown). On the contrary, the preincubation of the protein with 10 m*M* betaine resulted in an almost complete prevention of GST-GFP aggregation, even at 50°C [Fig. 3(A); AI ~1).

Protease accessibility to betaine-induced aggregates

The structural complexity of the protein aggregates formed in the presence of different betaine concentrations was investigated by the protease cleavage experiment. The fusion construct GST-GFP presents a TEV protease recognition site in the linker region between the two protein moieties.[23] The accessibility of TEV to its cleavage site is facilitated when the protein is in its correctly folded form or in loosely packed aggregates, while it is impaired in compact aggregates.[18] Interestingly, GST-GFP incubated in the presence of 6.6 m*M* betaine formed protease-resistant precipitates, while the protein preincubated in the absence and in the presence of 10 m*M* betaine was efficiently cleaved by TEV [Fig. 3(B)].

Disaggregation effect of betaine

The disaggregation capacity of betaine was investigated by DLS and turbidity measurements in a two-step experiment. First, GST-GFP aggregates were induced by either incubation in the presence of 6.6 m*M* betaine or by thermal treatment. Successively, further betaine was added and disaggregation of the already formed aggregates was observed.

As reported in previous paragraphs, the addition of 6.6 m*M* betaine induced the immediate formation of GST-GFP aggregates with Rh values of 52–3000 nm. When more betaine was added to this GST-GFP suspension at a final concentration of 10 m*M*, the protein precipitates were dissolved, the sample became transparent, its turbidity went back to the control value, and the Rh of the particles in solution decreased significantly [Fig. 2(C)]. Even though betaine was able to disassemble GST-GFP aggregates, the secondary structure of the dissolved protein was only partially recovered, while the tertiary structure was completely lost as shown by CD spectra [Fig. 2(A,B)].

Table II
Dynamic Light Scattering of GST-GFP Aggregates Induced by Thermal Treatment and Successively Incubated in the Presence of Betaine

Time	GST-GFP (10 m*M* betaine)	GST-GFP + heat shock (no betaine)	GST-GFP + heat shock + 10 m*M* betaine
0 min	Rh = 16.0 nm	Rh > 3,000 nm	Rh > 3,000 nm
50 min	Rh = 16.0 nm	Rh > 3,000 nm	Rh = 14.6 nm

GST-GFP protein was incubated for 15 min at 100°C in Tris HCl 20 m*M*, pH 8.0. The resulting thermal aggregates were resuspended in the same buffer in the absence and in the presence of 10 m*M* betaine. The hydrodynamic radius (Rh) of GST-GFP assemblies was estimated by dynamic light scattering measurements.

The disaggregation capacity of betaine was not limited to aggregates induced by betaine itself. In a previous article,[10] we showed that large aggregates formed after heating GST-GFP at 100°C for 15 min. These aggregates displayed Rh larger than 3000 nm, as identified by DLS analysis (Table II). After 50 min of incubation with 10 m*M* betaine, they disaggregated into particles having Rh of 14.6 nm.

DISCUSSION

We have recently described how the structural properties of GST-GFP protein aggregates depend on the physiological and experimental conditions in which the aggregation process takes place.[10] Here we show how betaine can tune, in a reproducible way, protein misfolding, aggregation, and disaggregation. In particular, we found that, when GST-GFP is incubated in the presence of betaine, a betaine-concentration-dependent effect on the protein structure and on its aggregation was observed. The structural and functional properties of GST-GFP in the presence of different betaine concentrations were detected by complementary methods, whose results are summarized in Table I. At low betaine concentrations, no detectable modifications of the protein structure were observed. At a critical concentration of betaine between 5 and 7.5 m*M*, the protein formed macroscopic aggregates [Fig. 1(A)] that, when analyzed by EM, were found to display large prefibrillar structures [Fig. 1(B)], characterized by subelements with a diameter of 50–100 nm. These aggregates bind the amyloid marker ThT, have Rhs in the range 50–3000 nm (Table I), and sediment at the lowest sucrose gradient interface [Fig. 1(C)]. Moreover, they appeared to be compact structures in which the TEV protease recognition site was not accessible [Fig. 3(B)]. Furthermore, the loss of the native secondary structures and the presence of intermolecular β-sheet protein–protein interactions within aggregates were observed by FTIR spectroscopy [Fig. 1(D)].

Different structural modifications on GST-GFP were found when the protein was incubated in the presence of higher betaine concentrations (10–20 m*M*). No green fluorescence, nor aggregation, were visible to the naked eye [Fig. 1(A)], indicating that the protein lost its tertiary structure, in agreement with the results of near-UV CD [Fig. 2(B)] and intrinsic fluorescence measurements (Table I). Moreover, small aggregates having diameter of 10–20 nm [Fig. 1(B)], Rh around 16 nm (Table I), and intermolecular β-sheet interaction [Fig. 1(D)] were detected by EM, DLS, and FTIR. The TEV digestion experiment [Fig. 3(B)] further indicated that the protein within these small aggregates was still accessible to the protease. All these results, therefore, indicate that 10–20 m*M* betaine misfolds the protein even more than 6.6 m*M* betaine, impairing high-order aggregation.

In addition to the concentration-dependent effect of betaine on protein misfolding and aggregation, the most important result reported here is that betaine can also disaggregate large and complex protein aggregates obtained under different conditions.

It should be noted that betaine addition (>10 m*M*) does not lead to the transformation of protein aggregates into unfolded monomers, as induced by chaotropic molecules, but into monodispersed assemblies of relatively large dimensions [Fig. 2(C) and Table II]. The soluble aggregates obtained by the direct addition of 10 m*M* betaine to the native GST-GFP solution displayed a Rh of about 16.0 nm (Table I). This value is lower than that found for soluble aggregates obtained at 10 m*M* betaine by the two-step experiment (first induction of aggregation by 6.6 m*M* betaine, then disaggregation of these precipitates by additional betaine up to 10 m*M*), as shown in Figure 2(C). This result indicates two different unfolding pathways in the two cases.

In addition, these soluble aggregates were found to be stable over long incubation times and, interestingly, to resist further aggregation induced by temperature [Fig. 3(A)].

Considering all these results, a mechanism for the betaine-concentration-dependent induction of protein misfolding, aggregation, and disaggregation can be proposed, in agreement with the recent advances on the osmolyte effects reported in the literature.[38–41]

The GST-GFP misfolding and aggregation induced by betaine can be explained by the balance of two different interactions.[38–41] The thermodynamically unfavorable interaction with the protein backbone, known as osmophobic effect,[38] is usually predominant and leads to protein stabilization. The thermodynamically favorable interaction of the osmolyte with the protein side chains has the opposite effect.[38–41] In the present case, the interaction of betaine with specific amino acid side chains, such as Phe and Trp,[41] seems to overcome the stabilizing osmophobic effect,[38] therefore leading to an overall GST-GFP destabilization. Moreover, it should be noted that, due to its polar structure, betaine could also screen charge iterations, preventing the stabilization of salt bridges with consequent destabilization of the protein structure [Fig. 1(B)]. Being misfolded, the protein is then

expected to aggregate. Indeed, at 5–7.5 m*M* betaine concentrations insoluble large aggregates were observed. At higher betaine concentration (10–20 m*M*), instead, soluble protein assemblies were formed. Actually, at this higher concentration the interaction of betaine with the side chains[41] of the misfolded GST-GFP further increased. Since this interaction induces a solubilization effect on the protein,[39] the higher osmolyte concentration, leading to higher protein solubility, is expected to inhibit the formation of large insoluble aggregates. In addition, it is interesting to note that the three betaine methyl groups could prevent hydrophobic protein–protein interactions, resulting in a reduced protein aggregation, in a similar way to what recently proposed for arginine.[42] Indeed, arginine was found to inhibit protein aggregation through the formation of hydrophobic surfaces by the alignment of its three methylene groups.[42]

Therefore, 10–20 m*M* betaine induces GST-GFP misfolding, the formation of soluble aggregates, and the disruption of large preformed protein aggregates into small soluble assemblies.

We should note that several effects on proteins have been recently reported for betaine even at low millimolar concentrations.[43,44] For instance, in the case of the intrinsically disordered α-synuclein, while 1*M* betaine was required to induce the folding of secondary structures, only 10 m*M* betaine was necessary to induce a change in the protein intrinsic fluorescence, that is in the protein tertiary structures.[43]

Protein destabilization has been rarely described in the literature for naturally occurring osmolytes. In particular, trimethylamine *N*-oxide (TMAO), as well as betaine, was observed to have a protein stabilizing effect at pH higher than their pK_as (4.66 for TMAO and 2.17 for betaine) and a destabilizing one at pH lower than the osmolyte pK_as.[45] Here, we actually report the GST-GFP destabilization effect of betaine at pH higher than its pK_a. Also trehalose has been found to destabilize the protein bromelain under thermal stress.[46]

Interestingly, a biphasic behavior has been reported for TMAO on the natively unfolded protein α-synuclein.[14] TMAO, at 1*M* concentration, induced a partial folding and aggregation of the protein, whereas at 3*M* concentration the formation of oligomers prevented further α-synuclein fibrillation. For betaine on GST-GFP, we also report here a biphasic behavior. At the low osmolyte concentration, the native structured protein undergoes a partial unfolding, followed by aggregation of its misfolded intermediate. Similarly, at high betaine concentrations, we observed the formation of soluble assemblies, preventing the formation of insoluble aggregates.

Considering all these results, it clearly appears that osmolytes can stabilize, misfold, aggregate, and disaggregate proteins depending on the balance between their unfavorable interaction with the protein backbone and their favorable interaction with side chains. Therefore, it must be expected that their overall effect is determined by the protein-specific amino acid sequence and by the physical/chemical properties of each osmolyte.[38–41,47]

Concerning the capacity of betaine at high concentration to disaggregate large protein aggregates, it is interesting to note that osmolytes can reach inside cells at several hundred millimolar concentrations.[48] In particular, the collaborative effect of osmolytes and molecular chaperones to prevent the aggregation of recombinant proteins *in vivo* has been demonstrated.[18] Interestingly, the results presented here could suggest an *in vivo* role for betaine in participating to the molecular chaperone activity during protein disaggregation.[21,22] Indeed, we showed that betaine can disassemble large insoluble aggregates into soluble assemblies with poor secondary and tertiary structure. These substrates would be more accessible to cellular chaperones and proteases, suggesting, therefore, that betaine could contribute to the *in vivo* recycling and degradation of proteins initially trapped into aggregates. We have previously shown[3] that the efficiency of *in vitro* chaperone-dependent refolding was inversely proportional to the aggregate complexity. It would be, therefore, interesting to explore whether betaine addition could improve the protein refolding by chaperons from complex aggregates.[21,22]

ACKNOWLEDGMENTS

The authors wish to thank D. Waugh for having provided the GST-GFP plasmid and Rachel Santarella for her assistance at the electronic microscope. A.N. acknowledges the postdoctoral fellowship of the University of Milano-Bicocca.

REFERENCES

1. Burg MB, Ferraris JD. Intracellular organic osmolytes: function and regulation. J Biol Chem 2008;283:7309–7313.
2. Ross CA, Poirier MA. Protein aggregation and neurodegenerative disease. Nat Med 2004;10:S10–S17.
3. Schrödel A, de Marco A. Characterization of the aggregates formed during recombinant protein expression in bacteria. BMC Biochem 2005;6:10.
4. Carrió M, Gonzalez-Montalban N, Vera A, Villaverde A, Ventura S. Amyloid-like properties of bacterial inclusion bodies. J Mol Biol 2005;347:1025–1037.
5. Chiti F, Webster P, Taddei N, Clark A, Stefani M, Ramponi G, Dobson CM. Designing conditions for *in vitro* formation of amyloid protofilaments and fibrils. Proc Natl Acad Sci USA 1999;96:3590–3594.
6. Dobson CM. Protein folding and misfolding. Nature 2003;426:884–890.
7. Zurdo J, Guijarro JL, Jimenez JL, Saibil HR, Dobson CM. Dependence on solution conditions of aggregation and amyloid formation by an SH3 domain. J Mol Biol 2001;311:325–340.
8. Calamai M, Canale C, Relini A, Stefani M, Chiti F, Dobson CM. Reversal of protein aggregation provides evidence for multiple aggregated states. J Mol Biol 2005;346:603–616.
9. Bieschke J, Zhang Q, Powers ET, Lerner RA, Kelly JW. Oxidative metabolites accelerate Alzheimer's amyloidogenesis by a two-step

mechanism, eliminating the requirement for nucleation. Biochemistry 2005;44:4977–4983.
10. Natalello A, Santarella R, Doglia SM, de Marco A. Physical and chemical perturbations induce the formation of protein aggregates with different structural features. Prot Expr Purif 2008;58: 356–361.
11. Ignatova Z, Gierasch LM. Inhibition of protein aggregation in vitro and in vivo by a natural osmoprotectant. Proc Natl Acad Sci USA 2006;103:13357–13361.
12. Arora A, Ha C, Park CB. Inhibition of insulin amyloid formation by small stress molecules. FEBS Lett 2004;564:121–125.
13. Kim YS, Cape SP, Chi E, Raffen R, Wilkins-Stevens P, Stevens FJ, Manning MC, Randolph TW, Solomon A, Carpenter JF. Counteracting effects of renal solutes on amyloid fibril formation by immunoglobulin light chains. J Biol Chem 2001;276:1626–1633.
14. Uversky VN, Li J, Fink AL. Trimethylamine-*N*-oxide-induced folding of alpha-synuclein. FEBS Lett 2001;509:31–35.
15. Yang DS, Yip CM, Huang TH, Chakrabartty A, Fraser PE. Manipulating the amyloid-beta aggregation pathway with chemical chaperones. J Biol Chem 1999;274:32970–32974.
16. Scaramozzino F, Peterson DW, Farmer P, Gerig JT, Graves DJ, Lew J. TMAO promotes fibrillization and microtubule assembly activity in the C-terminal repeat region of tau. Biochemistry 2006;45:3684–3691.
17. Roberts MF. Organic compatible solutes of halotolerant and halophilic microorganisms. Saline Systems 2005;1:5.
18. de Marco A, Vigh L, Diamant S, Goloubinoff P. Native folding of aggregation-prone recombinant proteins in *Escherichia coli* by osmolytes, plasmid- or benzyl alcohol-overexpressed molecular chaperones. Cell Stress Chaperones 2005;10:329–339.
19. Kharbanda KK, Mailliard ME, Baldwin CR, Sorrell MF, Tuma DJ. Accumulation of proteins bearing atypical isoaspartyl residues in livers of alcohol-fed rats is prevented by betaine administration: effects on protein-L-isoaspartyl methyltransferase activity. J Hepatol 2007;46:1119–1125.
20. Rontein D, Basset G, Hanson AD. Metabolic engineering of osmoprotectant accumulation in plants. Metab Eng 2002;4:49–56.
21. Goloubinoff P, Mogk A, Ben Zvi AP, Tomoyasu T, Bukau B. Sequential mechanism of solubilization and refolding of stable protein aggregates by a bichaperone network. Proc Natl Acad Sci USA 1999;96:13732–13737.
22. Mogk A, Deuerling E, Vorderwulbecke S, Vierling E, Bukau B. Small heat shock proteins, ClpB and the DnaK system form a functional triade in reversing protein aggregation. Mol Microbiol 2003;50:585–595.
23. Fox JD, Routzahn KM, Bucher MH, Waugh DS. Maltodextrin-binding proteins from diverse bacteria and archaea are potent solubility enhancers. FEBS Lett 2003;537:53–57.
24. Nominé Y, Ristriani T, Laurent C, Lefevre J-F, Weiss E, Travé G. A strategy for optimizing the monodispersity of fusion proteins: application to purification of recombinant HPV E6 oncoprotein. Protein Eng 2001;14:297–305.
25. LeVine H. Quantification of β-sheet amyloid fibril structures with thioflavin T. Methods Enzymol 1999;309:274–284.
26. Stegemann J, Ventzki R, Schrödel A, de Marco A. Comparative analysis of protein aggregates by blue native electrophoresis and subsequent SDS-PAGE in a three-dimensional geometry gel. Proteomics 2005;5:2002–2009.
27. Kelly SM, Jess TJ, Price NC. How to study proteins by circular dichroism. Biochim Biophys Acta 2005;1751:119–139.
28. Seshadri S, Khurana R, Fink AL. Fourier transform infrared spectroscopy in analysis of protein deposits. Methods Enzymol 1999; 309:559–576.
29. Barth A, Zscherp C. What vibrations tell us about proteins. Q Rev Biophys 2002;35:369–430.
30. Natalello A, Prokorov VV, Tagliavini F, Morbin M, Forloni G, Beeg M, Manzoni C, Colombo L, Gobbi M, Salmona M, Doglia SM. Conformational plasticity of the Gerstmann-Straussler-Scheinker disease peptide as indicated by its multiple aggregation pathways. J Mol Biol 2008;381:1349–1361.
31. Orsini F, Ami D, Villa AM, Sala G, Bellotti MG, Doglia SM. FT-IR microspectroscopy for microbiological stadies. J Microbiol Methods 2000;42:17–27.
32. Susi H, Byler DM. Resolution-enhanced Fourier transform infrared spectroscopy of enzymes. Methods Enzymol 1986;130:291–311.
33. Arrondo JLR, Goni FM. Structure and dynamics of membrane proteins as studied by infrared spectroscopy. Prog Biophys Mol Biol 1999;72:367–405.
34. Lim K, Ho JX, Keeling K, Gilliland GL, Ji X, Rüker F, Carter DC. Three-dimensional structure of *Schistosoma japonicum* glutathione *S*-transferase fused with a six-amino acid conserved neutralizing epitope of gp41 from HIV. Protein Sci 1994;3:2233–2244.
35. Ormo M, Cubitt AB, Kallio K, Gross LA, Tsien RY, Remington SJ. Crystal structure of the *Aequorea victoria* green fluorescent protein. Science 1996;273:1392–1395.
36. Natalello A, Ami D, Brocca S, Lotti M, Doglia SM. Secondary structure, conformational stability and glycosylation of a recombinant *Candida rugosa* lipase studied by Fourier-transform infrared spectroscopy. Biochem J 2005;385:511–517.
37. Natalello A, Doglia SM, Carey J, Grandori R. Role of flavin mononucleotide in the thermostability and oligomerization of *Escherichia coli* stress-defense protein WrbA. Biochemistry 2007;46:543–553.
38. Bolen DW, Baskakov IV. The osmophobic effect: natural selection of a thermodynamic force in protein folding. J Mol Biol 2001;310: 955–963.
39. Bolen DW. Effects of naturally occurring osmolytes on protein stability and solubility: issues important in protein crystallization. Methods 2004;34:312–322.
40. Ignatova Z, Gierasch LM. Effects of osmolytes on protein folding and aggregation in cells. Methods Enzymol 2007;428:355–372.
41. Auton M, Bolen DW. Predicting the energetics of osmolyte-induced protein folding/unfolding. Proc Natl Acad Sci USA 2005;102:15065–15068.
42. Das U, Hariprasad G, Ethayathulla AS, Manral P, Das TK, Pasha S, Mann A, Ganguli M, Verma AK, Bhat R, Chandrayan SK, Ahmed S, Sharma S, Kaur P, Singh TP, Srinivasan A. Inhibition of protein aggregation: supramolecular assemblies of arginine hold the key. Plos ONE 2007;11:e1176.
43. Hegde ML, Rao KS. DNA induces folding in alpha-synuclein: understanding the mechanism using chaperone property of osmolytes. Arch Biochem Biophys 2007;464:57–69.
44. Heffron JK, Moerland TS. Parvalbumin characterization from the euryhaline stingray *Dasyatis sabina*. Comp Biochem Physiol A Mol Integr Physiol 2008;150:339–346.
45. Singh R, Haque I, Ahmad F. Counteracting osmolyte trimethylamine *N*-oxide destabilizes proteins at pH below its pKa. Measurements of thermodynamic parameters of proteins in the presence and absence of trimethylamine *N*-oxide. J Biol Chem 2005;280: 11035–11042.
46. Habib S, Khan MA, Younus H. Thermal destabilization of stem bromelain by trehalose. Protein J 2007;26:117–124.
47. Harries D, Rosgen J. A practical guide on how osmolytes modulate macromolecular properties. Methods Cell Biol 2008;84:679–735.
48. Cayley S, Lewis BA, Record MT, Jr. Origins of the osmoprotective properties of betaine and proline in *Escherichia coli* K-12. J Bacteriol 1992;174:1586–1595.